Nano Energy 37 (2017) 168–176

Contents lists available at ScienceDirect

Nano Energy

journal homepage: www.elsevier.com/locate/nanoen

Full paper

Universal power management strategy for triboelectric nanogenerator

Fengben Xi[a,b,c,1], Yaokun Pang[a,b,c,1], Wei Li[a], Tao Jiang[a,b], Limin Zhang[a,b,c], Tong Guo[a], Guoxu Liu[a,b,c], Chi Zhang[a,b,*], Zhong Lin Wang[a,b,d,*]

[a] Beijing Institute of Nanoenergy and Nanosystems, Chinese Academy of Sciences, Beijing 100083, China
[b] National Center for Nanoscience and Technology (NCNST), Beijing 100190, China
[c] University of Chinese Academy of Sciences, Beijing 100049, China
[d] School of Material Science and Engineering, Georgia Institute of Technology, Atlanta, GA 30332, USA

ARTICLE INFO

Keywords:
Triboelectric nanogenerator
Power management
Buck conversion
Tribotronics
Power-tribotronics

ABSTRACT

Effective power management has always been the difficulty and bottleneck for practicability of triboelectric nanogenerator (TENG). Here we propose a universal power management strategy for TENG by maximizing energy transfer, direct current (DC) buck conversion, and self-management mechanism. With the implemented power management module (PMM), about 85% energy can be autonomously released from the TENG and output as a steady and continuous DC voltage on the load resistance. The DC component and ripple have been systematically investigated with different circuit parameters. At a low frequency of 1 Hz with the PMM, the matched impedance of the TENG has been converted from 35 MΩ to 1 MΩ at 80% efficiency, and the stored energy has been dramatically improved in charging a capacitor. The universality of this strategy has been greatly demonstrated by various TENGs with the PMM for harvesting human kinetic and environmental mechanical energy. The universal power management strategy for TENG is promising for a complete micro-energy solution in powering wearable electronics and industrial wireless networks. With the new coupling mode of triboelectricity and semiconductor in the PMM, the tribotronics has been extended and a new branch of power-tribotronics is proposed for manageable triboelectric power by electronics.

1. Introduction

With the rapid development of wearable electronics and sensor networks [1,2], batteries cannot meet the sustainable energy requirement due to the limited lifetime, heavy package and environmental pollution [3,4]. Ambient energy harvesting has attracted great attention in various forms, such as mechanical [5], solar [6], geothermal [7] and chemical [8]. Specifically, converting mechanical energy into electricity is considered as the most effective solution for the abundant existing in human and environment. Recent years, triboelectric nanogenerator (TENG) has been invented as a promising technology by harvesting mechanical energy [9–13], which is the application of Maxwell's displacement current in energy [14] and has demonstrated great advantages over traditional electromagnetic induction generator in light weight, low cost and low frequency [15–17]. The IDTechEx predicts that the triboelectric energy harvesting transducers will be a $400 million market in 2027. Up to now, the maximal output power of TENG has reached to 500 W/m^2 [18], which has shown great potentials as a sustainable energy technology. However, the TENG has very low efficiency in directly powering electronics and charging storages for the large impedance and unbalanced load matching [19,20]. Effective power management plays an essential role in efficient energy utilization of TENG, which has always been the difficulty and bottleneck for the practicability of TENG.

Over the past few years, many efforts have been made in power management for the TENG. Tang, Zi and et al. designed mechanical switches between serial-connected and parallel-connected capacitors for lowering the output voltage and enhancing the output charges [21,22]. Because of the complex mechanical layout, this design has limited the number of switch and transformer ratio. Zhu et al. introduced traditional transformer into the TENG and received the stable direct current (DC) output voltage [23], but this one only works in high-frequency and the customized transformer has a large size. Notably, Niu et al. proposed a self-charging system based on electronic switches and realized the random AC energy converting to DC electricity at 60% efficiency [24]. However, the power supply for electronic switches is to be stored and micro power cannot be managed for the large leakage in the circuit. Therefore, as a core technology for

* Corresponding authors at: Beijing Institute of Nanoenergy and Nanosystems, Chinese Academy of Sciences, Beijing 100083, China.
E-mail addresses: czhang@binn.cas.cn (C. Zhang), zlwang@gatech.edu (Z.L. Wang).
[1] These authors contributed equally to this work.

http://dx.doi.org/10.1016/j.nanoen.2017.05.027
Received 3 May 2017; Received in revised form 10 May 2017; Accepted 10 May 2017
Available online 12 May 2017

TENG, a universal, efficient and autonomous power management is highly expected for investigation.

Here in this work, we propose a power management strategy for TENG in theory and experiment, including maximized energy transfer, direct current (DC) buck conversion, and self-management mechanism. In the implemented power management module (PMM), a tribotronic energy extractor for TENG is developed and about 85% energy can be autonomously transferred. By coupling with the classical DC-DC buck converter, a steady and continuous DC voltage can be received on the load resistance and the output characteristics is systematically investigated with different circuit parameters. At a low frequency of 1 Hz with the PMM, the matched impedance of the TENG has been converted from 35 MΩ to 1 MΩ at 80% efficiency, and the stored energy has been dramatically improved a 1 mF capacitor. The PMM is compact in a size of 2×2×1 cm^3 and practical for various TENGs. The universal, efficient and autonomous power management strategy is validated for harvesting human kinetic and environmental mechanical energy, which has demonstrated promising prospects in powering wearable electronics and industrial wireless networks. Furthermore, this work exhibits manageable triboelectric power by electronics as a new coupling mode of triboelectricity and semiconductor, which can extend the tribotronics and derive out a new branch of power-tribotronics.

2. Results and discussion

2.1. Maximized energy transfer

The first step of the power management strategy is maximizing the energy transfer from the TENG to the back-end circuit. The operation process in one cycle is detailed in Fig. 1a. The TENG is selected in the freestanding sliding mode as a representative, which is made of a fluorinated ethylene propylene (FEP) film and two copper electrodes. The TENG is rectified and output by a serial switch for the back-end circuit, which is represented as a resistor. In the initial state, the voltage U and transferred charge Q of the TENG is starting from (Q, U) =(0, 0) and the switch is off. When the FEP film moves to the right end, Q is still zero and U reaches to the maximal value of U_{OC}. In this process, the energy is gradually accumulated to the maximum in the TENG. In state III, the switch is turned on and the energy from the TENG is releasing to the resistor in the path from node A to node B, along with the increasing Q and decreasing U, until Q reaches to the maximal value of Q_{SC} and U decreases to 0. The switch is turned off in state IV, and then the FEP film moves back to the left end in state V, in the process that the energy is accumulated again and U reaches to the negative maximal value of $-U'_{OC}$. The switch is tuned on again in state VI for energy releasing in the same path and then the process returns back to the initial state for a full cycle. The U-Q curve of the TENG in one cycle is plotted in Fig. 1b, which is corresponding with the previous studies that using a parallel switch to achieve maximized energy output cycle (CMEO) [25,26]. The difference is that the switch is in series after the rectifier for transferring the whole energy out of the TENG. The transferred energy to the resistor in one cycle can be described as:

$$E = \oint U dQ = \frac{1}{2} Q_{SC} (U_{OC} + U'_{OC}) \tag{1}$$

For each cycle of the TENG, the energy can be released to the resistor twice with similar process and difference in the initial releasing voltages. Fig. 1c has shown the schematic waveforms of the rectified voltage U_T of TENG and releasing voltage U_{AB} for the resistor. In the energy accumulation process during the period of t_2, U_T gradually increases to the maximal value of U_{OC} or U'_{OC}, and U_{AB} is zero. While

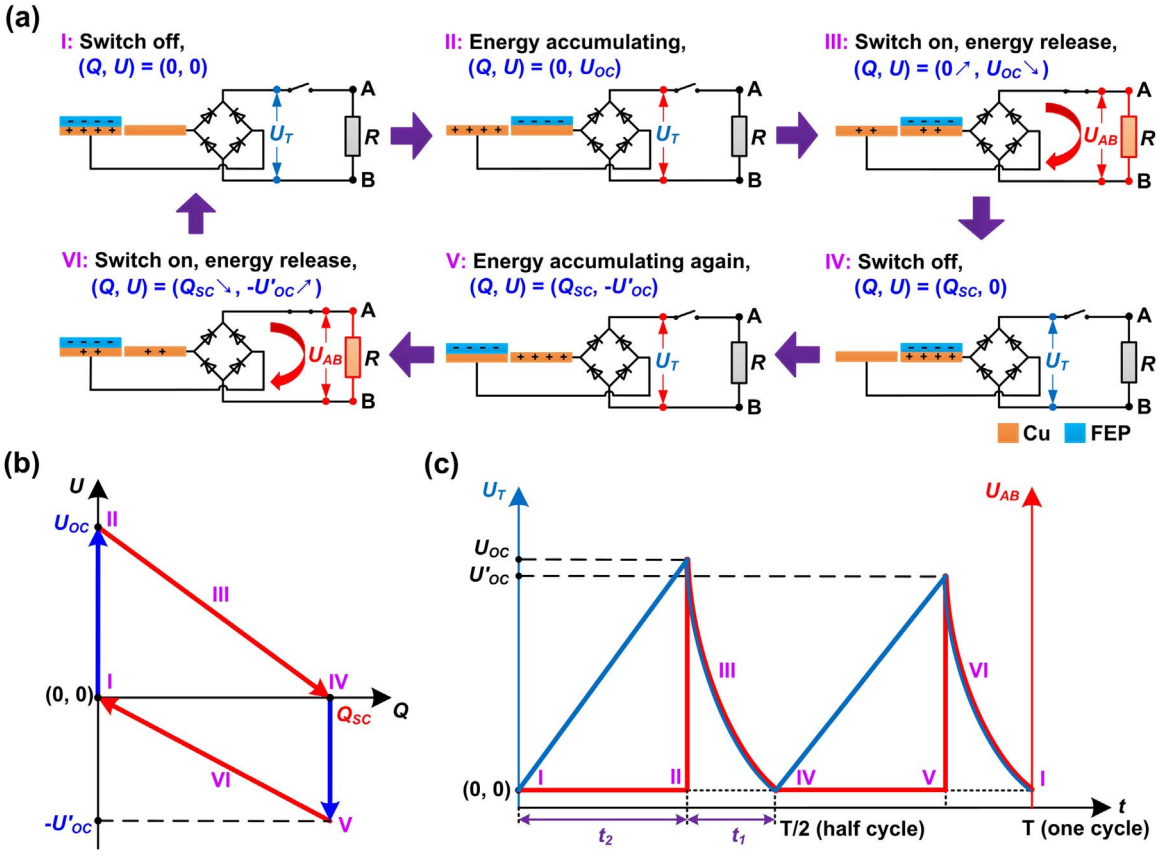

Fig. 1. Maximized energy transfer from TENG to a resistor. (a) Operating process in one cycle for releasing maximum energy from TENG and transferring it to a resistor by sequential switching. (b) The U-Q plot of the TENG in the maximized energy transfer cycle. (c) The schematic waveforms of the rectified voltage of TENG and the releasing voltage to the resistor, respectively.

in the energy release process during the period of t_1, U_{AB} is instantly rising up to the maximal value and then falls to zero in accordance with U_T. Therefore, the maximized energy transfer from the TENG is released to the back-end circuit with the interval pulse high voltage of U_{AB}.

The maximized energy transfer process has been experimentally demonstrated, based on a vertical contact-separation mode single-layer TENG in a size of 6.5 cm×5 cm, as shown in Fig. S1a (Supporting information). With the sequential mechanical switching in the cycle at 1 Hz, the *U-Q* curves with different resistances of 1 Ω, 100 kΩ and 1 MΩ are plotted and nearly coincident in Fig. S1b. Two cycles of U_T and U_{AB} waveforms with the resistance of 1 MΩ are shown in Fig. S1c and d, respectively. The two peak values of U_{AB} are about 300 V and 250 V, respectively. These experimental curves are in coincidence with the strategy analysis in Fig. 1, which has validated the maximized energy transfer characteristics.

2.2. DC buck conversion

Although the energy can be maximally transferred from the TENG, the interval pulse high voltage of U_{AB} still cannot directly supply for the electronics. On the basis of the circuit in Fig. 1a, the classical DC-DC buck converter is coupled as an AC-DC buck conversion circuit for the TENG, as shown in Fig. 2a. Between the switch and load resistor R, a parallel freewheeling diode D_1, a serial inductor L and a parallel capacitor C are added in sequence. The switch is used not only for the maximized energy transfer but also for DC buck conversion in the circuit.

In order to simplify the circuit analysis, we select the TENG in freestanding mode as shown in Fig. 1a, that a full cycle for the TENG with a symmetric structure can be considered as the same two circuit cycles. Each circuit cycle T_C has two periods (T_C=t_1+t_2) and the equivalent circuits are shown in Fig. 2b and c, respectively. When the switch is on during the period of t_1, the freewheeling diode is cutoff. The energy transfer is equivalent that a capacitor full of energy is discharging to the *LC* units. A part of energy is absorbed and stored in the inductor as the magnetic field energy and the other part of energy is stored in the capacitor as the electric field energy without energy dissipation. According to Kirchhoff's law, the releasing voltage $U_{AB}(t)$, inductor current $i_L(t)$ and output voltage $U_O(t)$ can be described as:

$$i_L(t) = i_C(t) + i_R(t) = C\frac{dU_O(t)}{dt} + \frac{U_O(t)}{R} \quad (2)$$

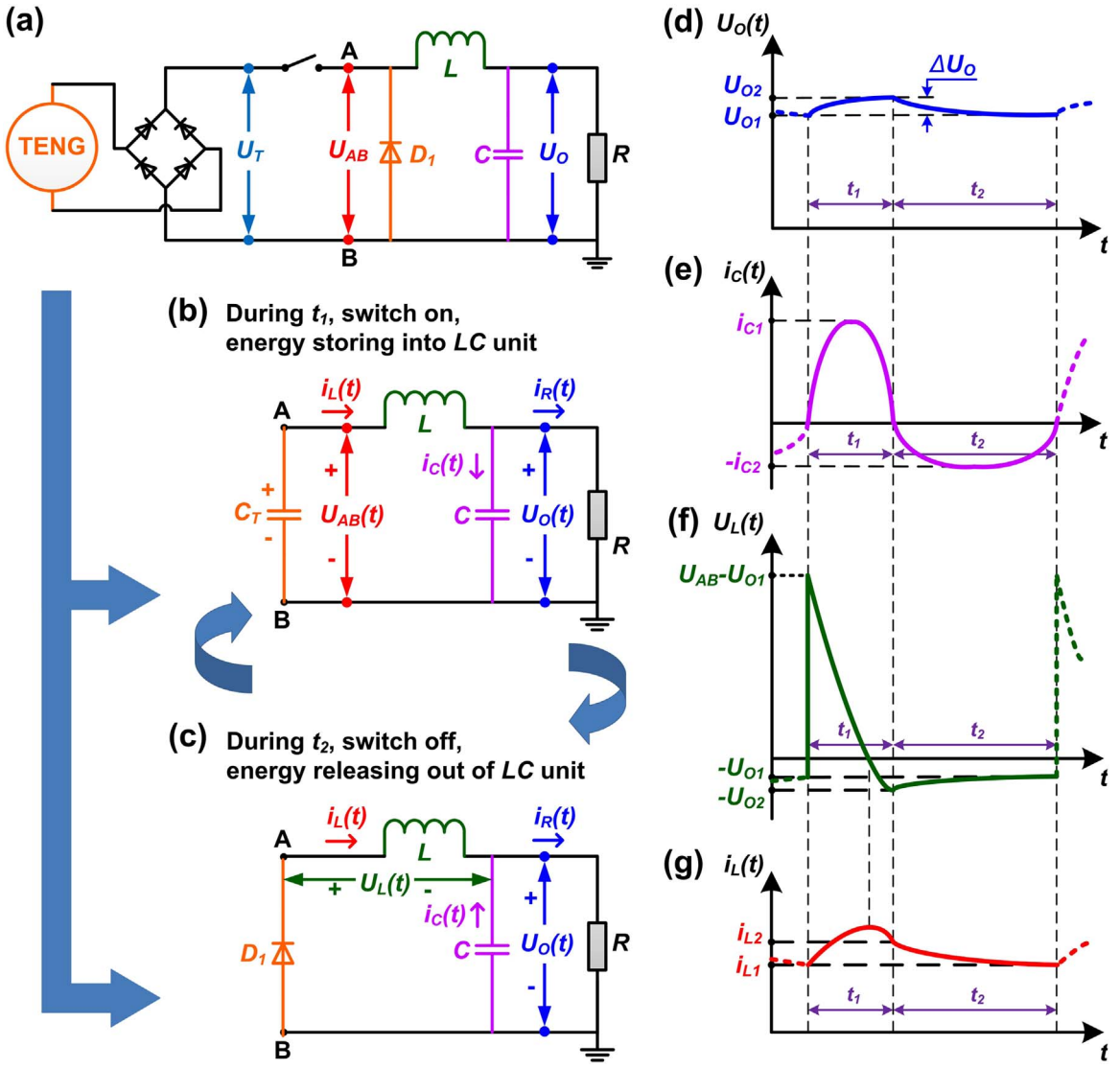

Fig. 2. AC-DC buck conversion for TENG. (a) The schematic circuit diagram of AC-DC buck conversion by coupling TENG, rectifier and classical DC-DC buck converter. (b) The equivalent circuit during switch on that the energy from TENG is storing into the *LC* units. (c) The equivalent circuit during switch off that the energy from TENG is releasing out of the *LC* units. (d–g) The schematic waveforms of (d) the output voltage on the resistor, (e) the capacitor current, (f) the inductor voltage, and (g) the inductor current in one circuit cycle.

$$U_L(t) = L\frac{di_L(t)}{dt} = U_{AB}(t) - U_O(t) \tag{3}$$

$$i_L(t) = C_T\frac{dU_{AB}(t)}{dt} \tag{4}$$

where the capacitor current $i_C(t)$, inductor voltage $U_L(t)$ and output current $i_R(t)$ are included. It is worth noting that the intrinsic capacitance C_T of the TENG is constant in freestanding mode and also a known periodic variable in other modes [27]. While when the switch is off during the period of t_2, the freewheeling diode is turned on as a loop for energy releasing from the inductor. The stored energies in *LC* units are both released to the load resistor. According to Kirchhoff's law and ignoring the voltage drop in diode, the inductor current $i_L(t)$ and output voltage $U_O(t)$ can also be described as:

$$i_L(t) = -i_C(t) + i_R(t) = -C\frac{dU_O(t)}{dt} + \frac{U_O(t)}{R} \tag{5}$$

$$U_L(t) = L\frac{di_L(t)}{dt} = -U_O(t) \tag{6}$$

In the alternating process, the output voltage $U_O(t)$ increases in the period of t_1 and decreases in the period of t_2. The average value is continuously rising from zero until achieving to a steady state that each circuit cycle has the same variation region. The steady state conditions are based on the principles of inductor volt-second balance and capacitor ampere-second balance as follow:

$$\frac{1}{T_C}\int_0^{T_C} U_L(t)dt = 0 \tag{7}$$

$$\frac{1}{T_C}\int_0^{T_C} i_C(t)dt = 0 \tag{8}$$

in which the average inductor voltage and capacitor current are both zero for each circuit cycle. Therefore, the above Eqs. (2)–(6) for two periods can be solved in the steady state with the particular conditions that $U_O(0)=U_O(T_C)=U_{O1}$, $U_O(t_1)=U_{O2}$, $i_L(0)=i_L(T_C)=i_{L1}$, $i_L(t_1)=i_{L2}$, $U_{AB}(0)=U_{OC}$, and $U_{AB}(t_1)=0$.

The characteristics of each variable for one circuit cycle in the steady state are schematically plotted in Fig. 2d–g, respectively. The results indicate that the output voltage $U_O(t)$ varies between U_{O1} and U_{O2} with a ripple of $\triangle U_O=U_{O2}-U_{O1}$. The capacitor current $i_C(t)$ rises from 0 to the maximum and then back to 0 in both periods with opposite directions. The inductor voltage $U_L(t)$ bumps up in the beginning and then declines and varies in negative region. The inductor current $i_L(t)$ also rises first and then falls. Consequently, the *LC* units in the circuit play a role of low pass filter, which has retained the DC component and restrained high frequency harmonic component in U_{AB}. By the strategy of DC buck conversion, the transferred energy from TENG can be achieved to a steady and continuous DC output voltage on the load resistor.

2.3. Self-management mechanism

The maximized energy transfer and DC buck conversion has elaborated the power management mechanism, in which the sequential control of the switch is essential for this strategy. To achieve the autonomous switching by the TENG with self-management mechanism, the switch is realized by a micro-power voltage comparator and a MOSFET, as shown in Fig. 3a. Driven by the TENG, the comparator is used to compare the rectified voltage U_T with the preset reference voltage U_{ref}. When U_T is less than U_{ref}, the comparator outputs a low level and the MOSFET is off. While when U_T exceeds U_{ref}, the comparator provides a high level to open the MOSFET for releasing

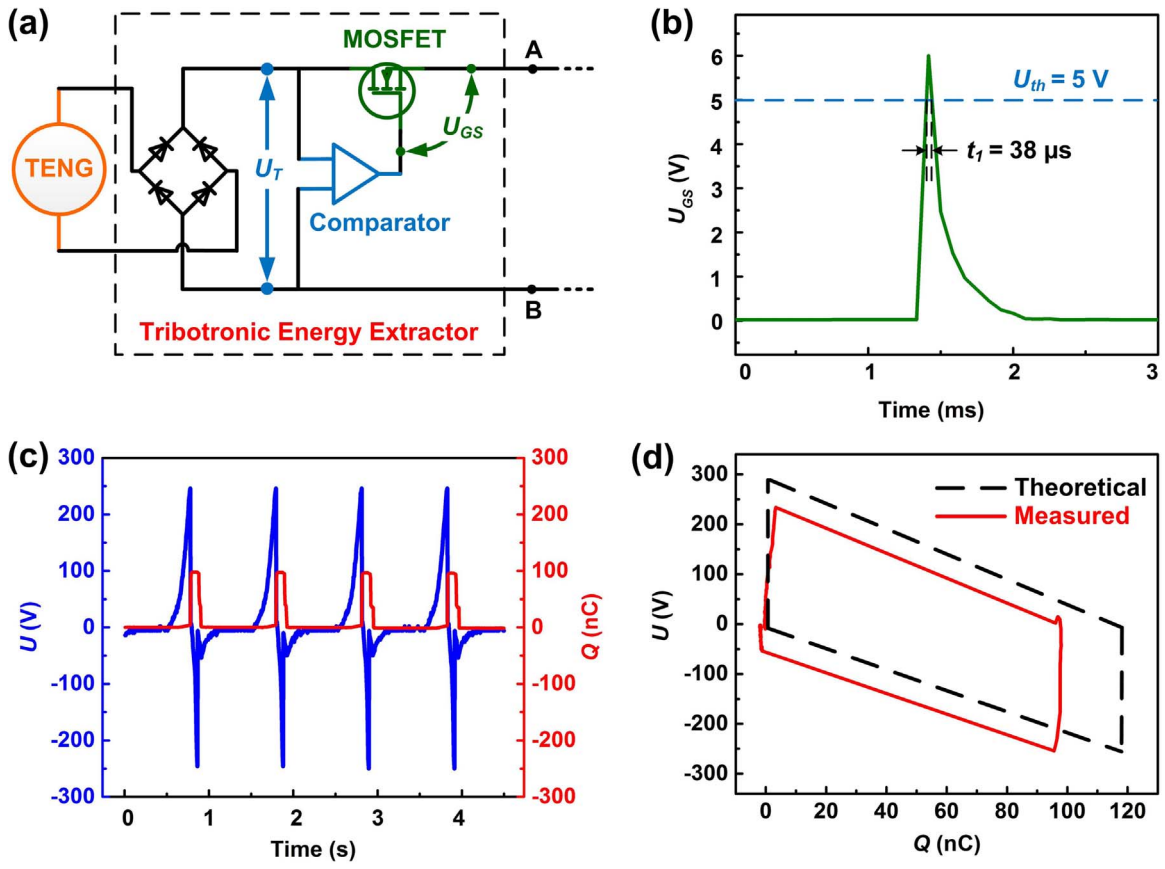

Fig. 3. Tribotronic energy extractor for autonomous energy transfer from the TENG. (a) The schematic circuit diagram of the tribotronic energy extractor (TEE) including the rectifier, a voltage comparator and a MOSFET switch. The energy is autonomously transferred by self-management mechanism without external power supply. (b) The voltage waveform U_{GS} by the comparator for controlling the MOSFET switch. (c) The *U*-*t* and *Q*-*t* plots of the TENG with the TEE. (d) The *U*-*Q* plot of the TENG by the TEE with 84.6% efficiency.

energy rapidly. By presetting U_{ref} according to U_{OC}, it can be realized that the switch is autonomously turned on when the voltage of TENG reaches to the peak and turned off when the energy is released, which is in accordance with the sequential switching in Fig. 1a. Based on the implemented autonomous switch and rectifier, a tribotronic energy extractor (TEE) is proposed. It can autonomously and maximally extract energy from the TENG and transfer to the back-end circuit without external power supply, which is a triboelectric power management device and much different from the previous tribotronics.

The characteristics of the TEE for the TENG in Fig. S1a are experimentally illustrated. Fig. 3b shows the voltage waveform U_{GS} by the comparator for controlling the MOSFET switch, which is a narrow pulse voltage within 1 ms. When the voltage exceeds the threshold voltage U_{th} of the MOSFET (5 V), the switch is turned on and the opening time t_1 is 38 μs for this controlling signal. It is worth noting that t_1 is much less than t_2 in the switching sequence, which is very suitable for the TENG in continuous periodic motion at low frequency. The U-t and Q-t plots of the TENG by the TEE are shown in Fig. 3c. At a low frequency of f=1 Hz, the voltage produces a series of pulse signals with steep falling edges and the transferred charge produces a series of step signals with both steep rising and falling edges, which has demonstrated the rapid energy releasing from the TENG. The peak voltage is about ± 250 V and the peak charge is about 100 nC. The U-Q curve is plotted in Fig. 3d for comparing the measurement result and the theoretical maximum in Fig. S1b. The comparison indicates that 84.6% energy can be autonomously transferred from the TENG by the TEE, with the error mainly due to the asymmetric structure of TENG, comparator parameters, and energy loss in the MOSFET. Therefore, the efficient TEE has validated the effective strategy of self-management mechanism for the TENG.

2.4. Characteristics of power management

With the strategy of maximized energy transfer, DC buck conversion, and self-management mechanism, the power management module (PMM) is implemented and characterized with the TENG. As shown in Fig. 4a, the U_O-t plot at f=1 Hz, R=1 MΩ, C=10 μF and L=5 mH is measured. The output voltage is continuously rising from the original state and reaches the steady state within 20 s. An enlarged view in the inset exhibits that the DC component is 3.0 V and the ripple is 0.4 V in the steady state. Obviously, the output characteristic accords with the theoretical analysis in Fig. 2d, which is very close to the voltage demands of the conventional electronics. When the load is connected with different resistors, the output voltages in the steady state are shown in Fig. 4b and summarized in Fig. 4c, respectively. It can be seen clearly that the DC component increases and the ripple decreases with the increasing resistance. Fig. 4d shows the average power curve with resistances in comparison with the direct output characteristic of the

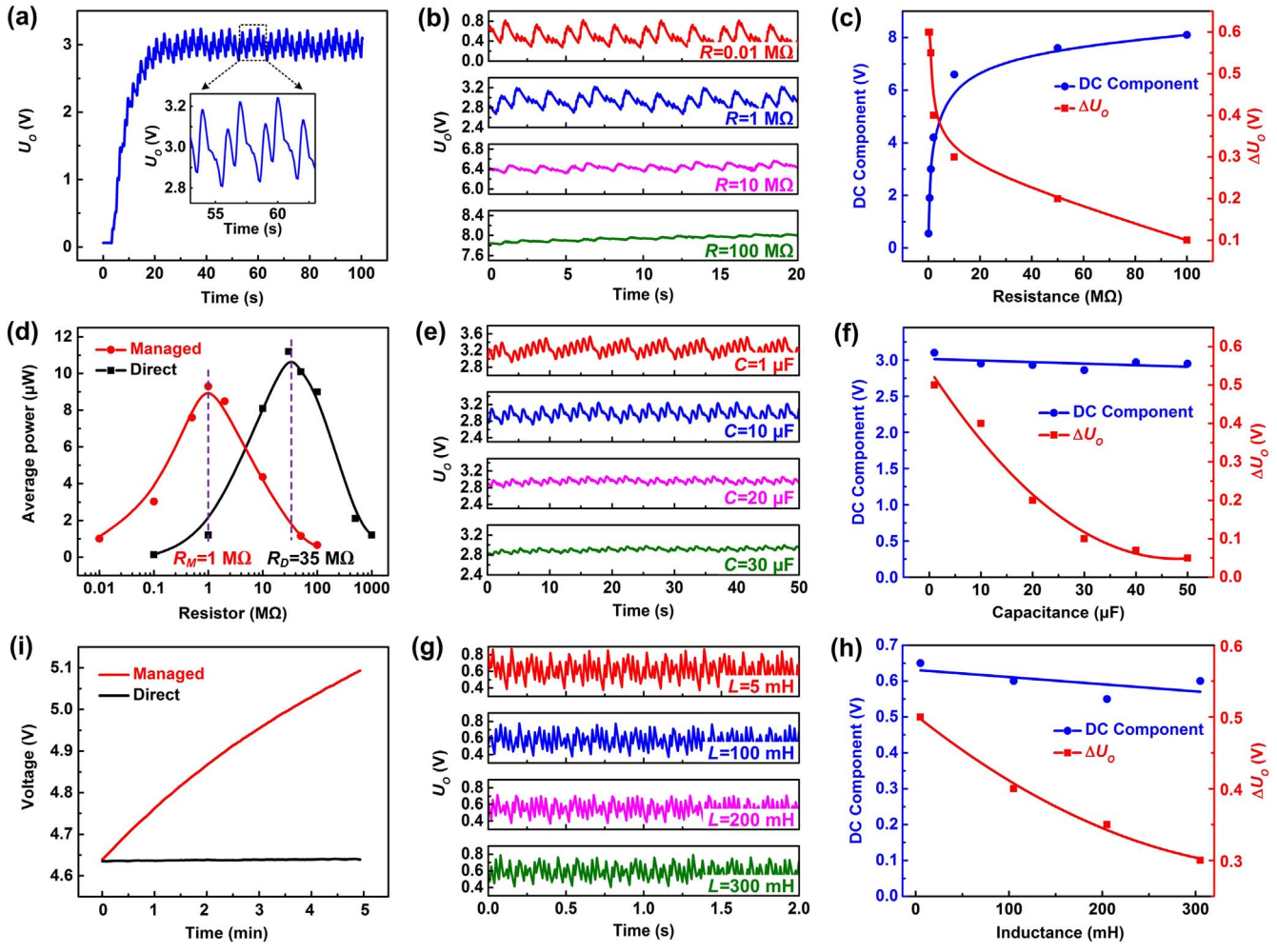

Fig. 4. Characteristics of the power management module (PMM) for TENG. (a) The measured U_O-t plot at f=1 Hz, R=1 MΩ, C=10 μF and L=5 mH. The response approaches steady state within 20 s. The inset shows the DC component is 3.0 V and the ripple is 0.4 V. (b) The measured U_O-t plot with different resistors. (c) The DC component and ripple of output voltage with different resistors. (d) Comparison of the direct and managed average power on external resistors, which shows the output impedance conversion by the PMM. (e) The measured U_O-t plot with different capacitances. (f) The DC component and ripple of output voltage with different capacitances. (g) The measured U_O-t plot with different inductances. (h) The DC component and ripple of output voltage with different inductances. (i) Comparison of direct and managed charging for a 1 mF capacitance.

TENG. At a low frequency of 1 Hz, the maximal average power directly from the TENG is 11.2 μW at the matched resistance of 35 MΩ. While the maximum is 9.0 μW with the PMM at the matched resistance of 1 MΩ, which indicates that the output impedance has been greatly reduced and the output power is retained at 80.4% efficiency.

The *LC* units are the important parameters in the PMM and have also been systematically investigated. The output voltage characteristics in the steady state are illustrated with the different capacitances at f=1 Hz, R=1 MΩ and L=5 mH in Fig. 4e and f, while with the different inductances at f=8 Hz, R=1 MΩ and C=10 μF in Fig. 4g and h. It can be seen clearly that the capacitance and inductance have nearly no effects on the DC components for the reason that neither of them are dissipating energy. However, the ripples both exhibit an obvious decrease with the increasing capacitance and inductance, which is because of their energy storage and filtering properties.

Besides the output characteristics for the load resistor, the charging curve for a 1 mF capacitance at 1 Hz is characterized in comparison with the direct charging by the TENG. As shown in Fig. 4i, by direct charging for 5 min, the voltage only increases from 4.632 V to 4.636 V with an increment of 18.5 μJ. While the voltage increases from 4.632 V to 5.118 V with an increment of 2.37 mJ by the PMM with 128 times improvement in stored energy. The dramatic contrast in capacitor charging is demonstrated by using the stored energy for driving a radio-frequency (RF) transmitter. The transmitter can send an on-off signal to a receiver 5–10 m away with about 200 μJ each time. A three layer TENG is used for directly charging a 22 μF capacitance without initial voltage and the stored energy in up to 100 cycles can drive the transmitter once. In comparison, charging with the PMM only for 5–10 cycles can exhibit the same result (Supplementary Movie 1).

Supplementary material related to this article can be found online at doi:10.1016/j.nanoen.2017.05.027.

2.5. Applications and universality

The implemented PMM has a compact package in size of 2×2×1 cm^3, which is very suitable for integrating with the various wearable TENGs and harvesting human kinetic energy. In Fig. 5a, we demonstrate four body motions at low frequency (~1 Hz) for powering different commercial electronic devices. In the first demo, a multilayer TENG is placed in an elbow pad and used for powering a common digital watch with the PMM. When an arm is gently bending for only once, the watch can be turned on and keep working for 15 s (Supplementary Movie 2). The second one demonstrates a woven TENG in clothes with the PMM for powering a digital thermometer. The thermometer is based on a thermistor and has no power in original state. With the arm swinging and clothes rubbing for 2–3 times, the thermometer starts to work and can constantly measure temperature with the continuous clothes rubbing (Supplementary Movie 3). A flexible TENG in a knee pad with the PMM is also demonstrated for powering a scientific calculator. The knee compressing back and forth

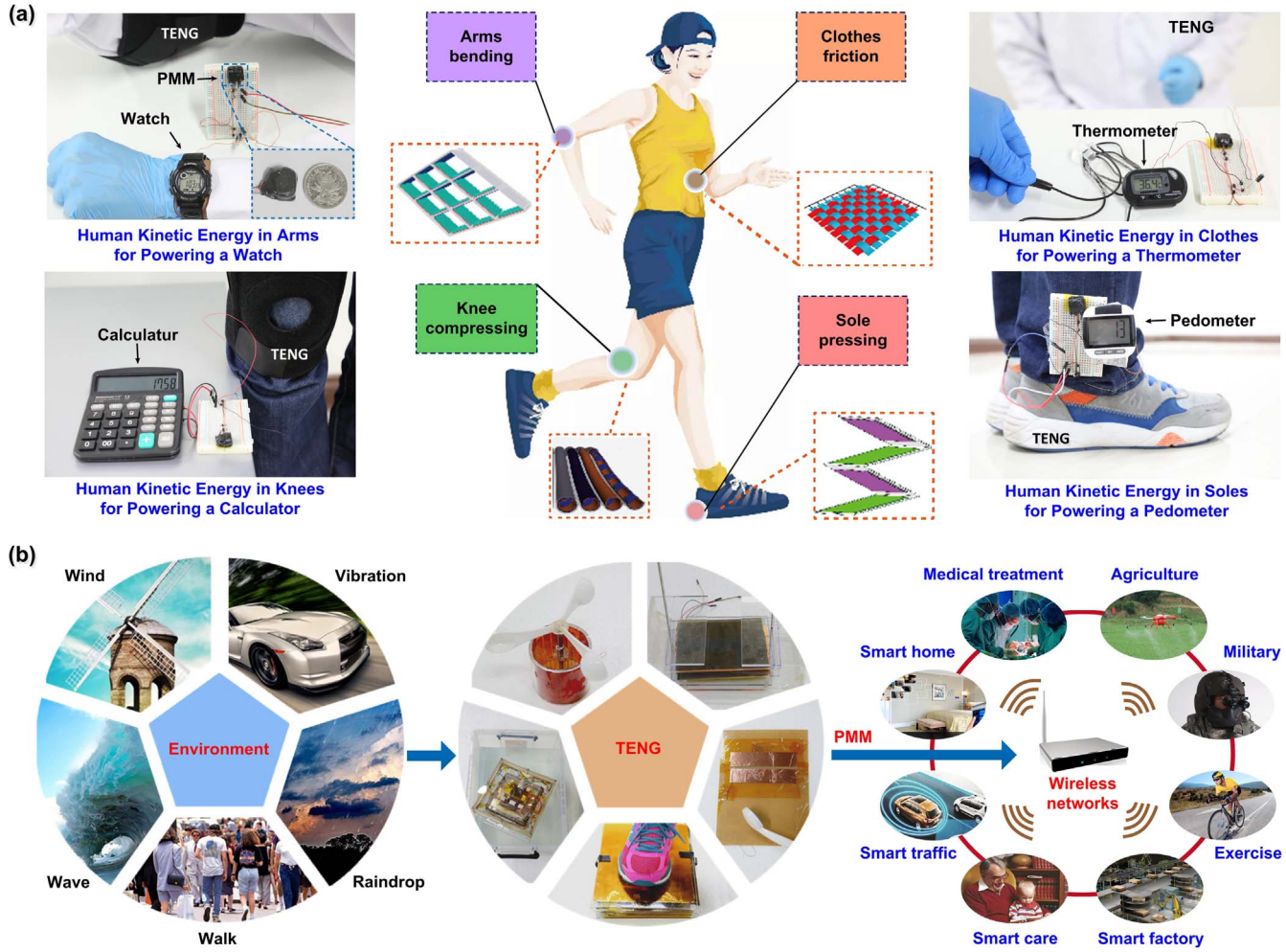

Fig. 5. Applications of harvesting human kinetic and environmental mechanical energy for demonstrating the universality of the power management strategy. (a) Human kinetic energy harvesting at low frequency (~1 Hz) by various wearable TENGs with the PMM, such as in arms, clothes, knees and soles for powering commercial electronic watch, thermometer, calculator and pedometer. (b) Environmental mechanical energy harvesting by various TENGs with the PMM, such as human walking, natural wind, vibration, wave and raindrop for distributed wireless sensor networks and future Energy Internet.

can quickly turn on the calculator and easily keep conventional calculation (Supplementary Movie 4). Furthermore, sole pressing with a folded TENG and the PMM is used for powering a pedometer. Without power in original state, 8 steps can start the pedometer and then steps can be counted and constantly displayed by continuous walking (Supplementary Movie 5).

Supplementary material related to this article can be found online at doi:10.1016/j.nanoen.2017.05.027.

Besides the human kinetic energy, various TENGs with the PMM can also be used for harvesting environmental mechanical energy, such as human walking, natural wind, vibration, wave and raindrop, as shown in Fig. 5b. In this work, the harvested energy is used for driving the RF transmitter. A pedal-TENG with the PMM is used for harvesting human walking energy, which are placed under the carpet. As one full cycle of the pedal-TENG with the PMM can provide above 200 μJ for the transmitter, a stamp on the carpet can realize the instantaneous wireless transmitting and trigger an alarm in the receiver (Supplementary Movie 6). In addition, several kinds of natural mechanical energy are simulated and harvested in a capacitor, respectively. With a wind-TENG and the PMM, the wind blowing in speed of 9 m/s for only 7 s can realize one RF transmission (Supplementary Movie 7). Similarly, with the PMM and other different TENGs, one RF transmission can also be realized by the structural vibration at 10 Hz for 15 s (Supplementary Movie 8), wave fluctuation at 2 Hz for 20 s (Supplementary Movie 9), and rainfall at 26 mL/s for 3 min (Supplementary Movie 10), respectively. Therefore, by harvesting human kinetic and environmental mechanical energy, the PMM has exhibited the universality of the power management strategy for various TENGs with different output capabilities, especially for tiny power management. The universal power management strategy for TENG is promising for a complete micro-energy solution for wearable electronics, distributed wireless sensor networks and future Energy Internet.

Supplementary material related to this article can be found online at doi:10.1016/j.nanoen.2017.05.027.

2.6. Power-tribotronics

As mentioned above, with the demonstrated TEE, the energy of the TENG has been maximally transferred by the autonomous electronic switch. And with the proposed power management strategy, the output characteristics of TENG have successfully managed by a series of electronic devices. They have both exhibited management effects on triboelectricity by electronics, which is a new coupling mode of triboelectricity and semiconductor. We call this power-tribotronics, which is an extension and new branch of tribotronics. Just as electronics contains information-electronics and power-electronics, the complete tribotronics can also be divided into information tribotronics (info-tribotronics) and power-tribotronics, as shown in Fig. 6a. The previous tribotronics, such as tribotronic transistor [28,29], contact-gated OLED [30], touch memory [31], wind-enhanced photocell [32], sliding tunable diode [33], and tactile sensing array [34], have all demonstrated controlled electronics by triboelectric potential for information sensing and active control [35–40], which are belonging to info-tribotronics. On the other hand, the power-tribotronics can demonstrate manageable triboelectric power by electronics for power management and efficient utilization, such as the TEE and the PMM in this work, and many potential devices for triboelectricity in the future. The comparison and distinction of info-tribotronics and power-tribotronics are shown in Fig. 6b. Therefore, we can update the definition of tribotronics in the whole scope. Tribotronics is about the research on interaction between triboelectricity and semiconductor, which is using triboelectric potential controlling electrical transport and transformation in semiconductors for information sensing and active control, and using semiconductors managing triboelectric power transfer and conversion in circuits for power management and efficient utilization.

3. Conclusion

In summary, we have proposed a universal power management strategy for TENG by maximizing energy transfer, DC buck conversion, and self-management mechanism. With the implemented TEE and PMM, about 85% energy can be autonomously released from the TENG and output as a steady and continuous DC voltage on the load resistance. The output characteristics have been systematically investigated with different circuit parameters. At a low frequency of 1 Hz with the PMM, the matched impedance of the TENG has been converted from 35 MΩ to 1 MΩ at 80% efficiency, and the stored energy has been improved by 128 times in charging a 1 mF capacitor. The PMM is compact and practical for various TENGs. The universality of this strategy has been greatly demonstrated for harvesting human kinetic and environmental mechanical energy, which is promising for a complete micro-energy solution for wearable electronics, distributed wireless sensor networks and future Energy Internet. Furthermore, this work has exhibited manageable triboelectric power by electronics as a new coupling mode of triboelectricity and semiconductor, which has extended the tribotronics and derived out a new branch of power-tribotronics.

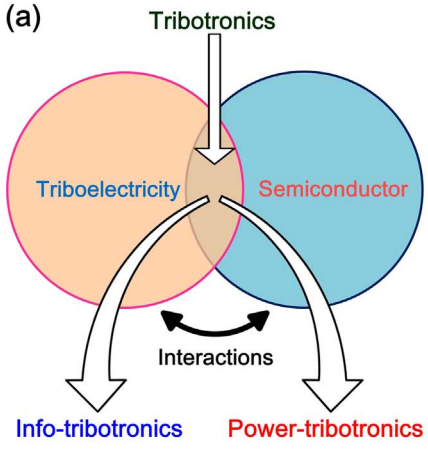

(b)

	Info-tribotronics	Power-tribotronics
Mechanism	Triboelectric potential controlling semiconductors	Semiconductors managing triboelectric power
Functions	Information sensing and active control	Power management and efficient utilization
Typical devices	Tribotronic transistor, tribotronic OLED, tribotronic memory, tribotronic phototransistor, tribotronic tuning diode, tribotronic tactile array, ...	Tribotronic switch, tribotronic energy extractor, tribotronic voltage converter, tribotronic charge amplifier, tribotronic power regulator, tribotronic energy networks, ...
Applications	Human/environmental interfacing, sensors, MEMS, flexible electronics, ...	Portable electronics, wireless sensor network, Internet of Things, blue energy, ...

Fig. 6. Formation and extension of tribotronics. (a) Schematic diagrams showing tribotronics by coupling between triboelectricity and semiconductor, which derives out info-tribotronics and power-tribotronics. (b) Comparison and distinction of info-tribotronics and power-tribotronics in mechanism, functions, typical devices, and applications. Plenty of typical and potential devices in power-tribotronics are presented.

Acknowledgments

The authors thank the support of National Natural Science Foundation of China (No. 51475099), Beijing Natural Science Foundation (No. 4163077), Beijing Nova Program (No. Z171100001117054), the Youth Innovation Promotion Association, CAS (No. 2014033), the "thousands talents" program for the pioneer researcher and his innovation team, China, and National Key Research and Development Program of China (2016YFA0202704). The authors also thank Liang Xu, Wei Tang, Junqing Zhao, Xianpeng Fu, Zhiwei Yang, Tianzhao Bu and Bo Wu for TENGs fabrication and applications demonstration.

Appendix A. Supporting information

Supplementary data associated with this article can be found in the online version at doi:10.1016/j.nanoen.2017.05.027.

References

[1] J.A. Rogers, T. Someya, Y. Huang, Science 327 (2010) 1603–1607.
[2] H.H. Chou, A. Nguyen, A. Chortos, J.W.F. To, C. Lu, J. Mei, T. Kurosawa, W.G. Bae, J.B.H. Tok, Z. Bao, Nat. Commun. 6 (2015) 8011.
[3] J.M. Tarascon, M. Armand, Nature 414 (2001) 359–367.
[4] Z.L. Wang, Faraday Discuss. 176 (2014) 447–458.
[5] S.P. Beeby, M.J. Tudor, N.M. White, Meas. Sci. Technol. 17 (2006) 175–195.
[6] D.J. Burke, D.J. Lipomi, Energy Environ. Sci. 6 (2013) 2053–2066.
[7] J.W. Lund, D.H. Freeston, Geothermics 30 (2001) 29–68.
[8] M.S. Dresselhaus, G. Chen, M.Y. Tang, R.G. Yang, H. Lee, D., Z. Wang, Z.F. Ren, J.P. Fleurial, P. Gogna, Adv. Mater. 19 (2007) 1043–1053.
[9] F.R. Fan, Z.Q. Tian, Z.L. Wang, Nano Energy 1 (2012) 328–334.
[10] T. Zhou, C. Zhang, C.B. Han, F.R. Fan, W. Tang, Z.L. Wang, ACS Appl. Mater. Interfaces 6 (2014) 14695–14701.
[11] T. Zhou, L. Zhang, F. Xue, W. Tang, C. Zhang, Z.L. Wang, Nano Res. 9 (2016) 1442–1451.
[12] C.B. Han, C. Zhang, J. Tian, X. Li, L. Zhang, Z. Li, Z.L. Wang, Nano Res. 8 (2014) 219–226.
[13] L.M. Zhang, C.B. Han, T. Jiang, T. Zhou, X.H. Li, C. Zhang, Z.L. Wang, Nano Energy 22 (2016) 87–94.
[14] Z.L. Wang, Mater. Today 20 (2017) 74–82.
[15] C. Zhang, W. Tang, C. Han, F. Fan, Z.L. Wang, Adv. Mater. 26 (2014) 3580–3591.
[16] F.R. Fan, W. Tang, Y. Yao, J.J. Luo, C. Zhang, Z.L. Wang, Nanotechnology 25 (2014) 135402.
[17] Y. Zi, H. Guo, Z. Wen, M.H. Yeh, C. Hu, Z.L. Wang, ACS Nano 10 (2016) 4797–4805.
[18] G. Zhu, Y.S. Zhou, P. Bai, X.S. Meng, Q. Jing, J. Chen, Z.L. Wang, Adv. Mater. 26 (2014) 3788–3796.
[19] W. Tang, C. Zhang, C.B. Han, Z.L. Wang, Adv. Funct. Mater. 24 (2014) 6684–6690.
[20] X. Pu, M.M. Liu, L.X. Li, C. Zhang, Y.K. Pang, C.Y. Jiang, L.H. Shao, W.G. Hu, Z.L. Wang, Adv. Sci. 1 (2016) 1500255.
[21] W. Tang, T. Zhou, C. Zhang, F.R. Fan, C.B. Han, Z.L. Wang, Nanotechnology 25 (2014) 225402.
[22] Y. Zi, H. Guo, J. Wang, Z. Wen, S. Li, C. Hu, Z.L. Wang, Nano Energy 31 (2016) 302–310.
[23] G. Zhu, J. Chen, T. Zhang, Q. Jing, Z.L. Wang, Nat. Commun. 5 (2014) 3426.
[24] S. Niu, X. Wang, F. Yi, Y.S. Zhou, Z.L. Wang, Nat. Commun. 6 (2015) 8975.
[25] Y. Zi, S. Niu, J. Wang, Z. Wen, W. Tang, Z.L. Wang, Nat. Commun. 6 (2015) 8376.
[26] Y. Zi, J. Wang, S. Wang, S. Li, Z. Wen, H. Guo, Z.L. Wang, Nat. Commun. 7 (2016) 10987.
[27] S. Niu, Z.L. Wang, Nano Energy 14 (2014) 161–192.
[28] C. Zhang, W. Tang, L. Zhang, C. Han, Z.L. Wang, ACS Nano 8 (2014) 8702–8709.
[29] Y.K. Pang, J. Li, T. Zhou, Z.W. Yang, J.J. Luo, L.M. Zhang, G.F. Dong, C. Zhang, Z.L. Wang, Nano Energy 31 (2017) 533–540.
[30] C. Zhang, J. Li, C.B. Han, L.M. Zhang, X.Y. Chen, L.D. Wang, G.F. Dong, Z.L. Wang, Adv. Funct. Mater. 25 (2015) 5625–5632.
[31] J. Li, C. Zhang, L. Duan, L.M. Zhang, L.D. Wang, G.F. Dong, Z.L. Wang, Adv. Mater. 28 (2016) 106–110.
[32] C. Zhang, Z.H. Zhang, X. Yang, T. Zhou, C.B. Han, Z.L. Wang, Adv. Funct. Mater. 26 (2016) 2554–2560.
[33] T. Zhou, Z.W. Yang, Y.K. Pang, L. Xu, C. Zhang, Z.L. Wang, ACS Nano 11 (2017) 882–888.
[34] Z.W. Yang, Y.K. Pang, L. Zhang, C. Lu, J. Chen, T. Zhou, C. Zhang, Z.L. Wang, ACS Nano 10 (2016) 10912–10920.
[35] C. Zhang, Z.L. Wang, Nano Today 11 (2016) 521–536.
[36] C. Zhang, L.M. Zhang, W. Tang, C.B. Han, Z.L. Wang, Adv. Mater. 27 (2015) 3533–3540.
[37] F. Xue, L.B. Chen, L.F. Wang, Y.K. Pang, J. Chen, C. Zhang, Z.L. Wang, Adv. Funct. Mater. 26 (2016) 2104–2109.
[38] Y.K. Pang, F. Xue, L.F. Wang, J. Chen, J.J. Luo, T. Jiang, C. Zhang, Z.L. Wang, Adv. Sci. 3 (2016) 1500419.
[39] L.M. Zhang, Z.W. Yang, Y.K. Pang, T. Zhou, C. Zhang, Z.L. Wang, Nano Res. (2017). http://dx.doi.org/10.1007/s12274-017-1564-9.
[40] Y.K. Pang, Li. Bo Chen, G.F. Hu, J.J. Luo, Z.W. Yang, C. Zhang, Z.L. Wang, Nano Res. (2017). http://dx.doi.org/10.1007/s12274-017-1599-y.

Fengben Xi received his undergraduate degree in Electronic Information Engineering from Shandong Normal University, China in 2014. He is currently pursuing his master degree in the Beijing Institute of Nanoenergy and Nanosystems, Chinese Academy of Sciences. His research interests are mainly focused on triboelectric nanogenarator and tribotronics, especially focus on the power management, tribotronic transistor and their applications in sensor networks and human machine interaction.

Yaokun Pang received his undergraduate degree from Qingdao University in 2013, and now he is a doctoral candidate in Beijing Institute of Nanoenergy and Nanosystems, Chinese Academy of Sciences. His research interests are triboelectric nanogenerator, flexible electronic, semiconductors and their applications in self-powered sensor networks and human-machine interaction.

Prof. Wei Li received his undergraduate degree from the Department of Automation Engineering, Northwestern Polytechnical University in 1986. He worked in AVIC Beijing Aeronautical Manufacturing Technology Research Institute and Intelligent Micro-system Research Laboratory of Tsinghua University. Currently, he joined Beijing Institute of Nanoenergy and Nanosystems, Chinese Academy of Sciences as a visiting fellow. His research focuses on the usability tests and verification of commercial devices on micro-nano spacecraft, the data acquisition and transmission technology for ultra-low-power sensors, and the collection and management technology of micro-nano energy.

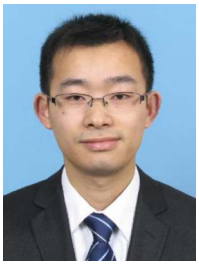

Dr. Tao Jiang received his Ph.D. degree from East China University of Science and Technology in 2014. Now he is an associate researcher in Prof. Zhong Lin Wang's group at the Beijing Institute of Nanoenergy and Nanosystems, Chinese Academy of Sciences. His research interests are the theoretical studies of triboelectric nanogenerators, and practical applications in self-powered sensing and blue energy harvesting.

Limin Zhang received her undergraduate degree from Hebei University of Technology in 2012, and now she is a doctoral candidate. Her research interests are piezoelectric nanogenerator and triboelectric nanogenerator, especially focus on triboelectricity based active micro/nano-sensors, flexible electronics, tribotronic circuit and their applications in sensor networks and human machine interaction.

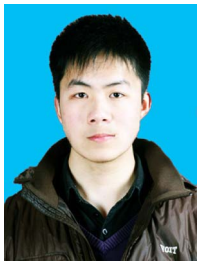

Tong Guo received his undergraduate degree in Physics from Zhengzhou University in 2016, and now he is a graduate student in Zhengzhou University and visiting student in Beijing Institute of Nanoenergy and Nanosystems, Chinese Academy of Sciences. His research interests are focused on triboelectric nanogenerator, hall elements, and their applications in sensor networks.

Guoxu Liu received his master degree in material science engineering from Tianjin University of Technology in 2016. Now he is a Ph.D. student at Beijing Institute of Nanoenergy and Nanosystems, Chinese Academic Science. His current research mainly focuses on energy harvesting and fabrication of nanodevices.

Prof. Chi Zhang received his Ph.D. degree from Tsinghua University in 2009. After graduation, he worked in Tsinghua University as a postdoc research fellow and NSK Ltd., Japan as a visiting scholar. He now is the principal investigator of Tribotronics Group in Beijing Institute of Nanoenergy and Nanosystems, Chinese Academy of Sciences (CAS), Fellow of the NANOSMAT Society, Member of Youth Innovation Promotion Association, CAS, and Youth Working Committee Member of Chinese Society of Micro-Nano Technology. Prof. Chi Zhang's research interests are triboelectric nanogenerator, tribotronics, self-powered MEMS/NEMS, and applications in sensor networks, human-computer interaction and new energy technology. He has been awarded by NSK Sino-Japan Friendship Excellent Paper Award of Mechanical Engineering and granted by National Natural Science Foundation of China, Beijing Municipal Science & Technology Commission, Beijing Natural Science Foundation, China Postdoctoral Science Foundation, and CAS. He has published over 60 papers and attained 15 patents.

Prof. Zhong Lin (ZL) Wang received his Ph.D from Arizona State University in physics. He now is the Hightower Chair in Materials Science and Engineering, Regents' Professor, Engineering Distinguished Professor and Director, Center for Nanostructure Characterization, at Georgia Tech. Dr. Wang has made original and innovative contributions to the synthesis, discovery, characterization and understanding of fundamental physical properties of oxide nanobelts and nanowires, as well as applications of nanowires in energy sciences, electronics, optoelectronics and biological science. His discovery and breakthroughs in developing nanogenerators established the principle and technological road map for harvesting mechanical energy from environment and biological systems for powering a personal electronics. His research on self-powered nanosystems has inspired the worldwide effort in academia and industry for studying energy for micro-nano-systems, which is now a distinct disciplinary in energy research and future sensor networks. He coined and pioneered the field of piezotronics and piezo-phototronics by introducing piezoelectric potential gated charge transport process in fabricating new electronic and optoelectronic devices. Details can be found at: www.nanoscience.gatech.edu.